Journal of Immunological Methods 472 (2019) 16–24

Contents lists available at ScienceDirect

Journal of Immunological Methods

journal homepage: www.elsevier.com/locate/jim

Comparative analysis of the germinal center response by flow cytometry and immunohistology

Gustaf Lindgren[a,b], Sebastian Ols[a,b], Elizabeth A. Thompson[a,b], Karin Loré[a,b,*]

[a] Division of Immunology and Allergy, Department of Medicine Solna, Karolinska Institutet and Karolinska University Hospital, Sweden
[b] Center for Molecular Medicine, Karolinska Institutet, Stockholm, Sweden

ARTICLE INFO

Keywords:
Germinal center
Vaccine
Non-human primate
Lymph nodes

ABSTRACT

Germinal centers (GCs) are structures formed within B cell follicles critical for the generation of high affinity antibodies. The evaluation of GCs in secondary lymphoid tissues has emerged as a valuable means for understanding the immunological activity in vaccine responses, autoimmunity and cancer. The analysis has been facilitated by advances in sampling techniques, including non-invasive lymph node collection and fine needle aspiration. In this study, we performed a systematic comparison between immunohistology and flow cytometry for analysis of GCs with the major aim to identify strategies for data analysis that would allow to relate data acquired by the two methods. Lymph nodes from rhesus macaques were divided in half and analysed as either cryosections or cell suspensions. Using human markers such as PD-1 and Ki67 to identify T follicular helper (T_{FH}) cells and GC B cells, we developed a method for GC analysis by immunohistology using CellProfiler™ software and a flow cytometry panel with relatively limited numbers of antibodies to be scalable and feasible for most laboratories to perform. While some discrepancies between the two methods were identified, T_{FH} cells and GC B cells normalized by total $CD3^+$ T cell or $CD20^+$ B cell numbers, respectively, in immunohistology correlated well with matched data from flow cytometry. GC area normalized by section area in immunohistology also correlated well with T_{FH} cells per total live cells from flow cytometry. Performing this type of data analysis would therefore facilitate comparison of results generated between the two methods.

1. Introduction

Germinal centers (GCs) are sub-anatomical structures located in secondary lymphoid organs, comprised of three main cell subsets; T follicular helper (T_{FH}) cells, GC B cells, and follicular dendritic cells (Willard-Mack, 2006). While follicular dendritic cells provide a scaffold to maintain antigen within the GC, T_{FH} cells are present to select B cells with high affinity B cell receptors (BCRs) for survival, proliferation and differentiation (Victora and Nussenzweig, 2012). Structurally, the GC can be divided into a dark zone where B cells proliferate and a light zone where high affinity B cells are selected in a T_{FH} cell-dependent manner (Mesin et al., 2016). GC B cells can be distinguished from their non-GC counterparts by their expression of the nuclear protein Ki67, the transcription factor BCL6 and their specific location within the lymph node (LN) (Victora and Nussenzweig, 2012; Mesin et al., 2016; Sobecki et al., 2016; Couillault et al., 2018). T_{FH} cells express the chemokine receptor CXCR5, responsible for migration to the light zone following a CXCL13 chemokine gradient (Schaerli et al., 2000; Havenar-Daughton et al., 2016a). T_{FH} cells also highly express programmed death receptor 1 (PD-1), which controls their positioning within the LN and prevents over-activation (Shi et al., 2018). Additionally, the inducible costimulatory molecule (ICOS) receptor is highly expressed on T_{FH} cells, and upon activation increases BCL6 expression which shapes the T_{FH} cell phenotype (Couillault et al., 2018; Choi et al., 2011a,b).

The GC reaction is central in regulating immunity and its activity is therefore a key component in conditions such as in cancer and autoimmunity or the responses to vaccination (Domeier et al., 2017; Kuppers, 2005; Doria-Rose and Joyce, 2015). Mutations in the BCR are the source of most lymphomas, which are almost exclusively GC B cell derived (Kuppers, 2005). In addition, highly mutated GC B cell clones with high affinity BCRs towards vaccine antigens are the end goal for most vaccine strategies (Doria-Rose and Joyce, 2015). Conversely, in autoimmune settings, GC B cells react to self-antigens and produce auto-antibodies that cause disease (Domeier et al., 2017). Due to this central role in immunity, the formation of GCs in lymphoid organs from experimental animal models and patients are frequently analysed.

The most common methods of GC analysis to date are

* Corresponding author at: Division of Immunology and Allergy, Department of Medicine Solna, Karolinska Institutet and Karolinska University Hospital, Sweden
E-mail address: karin.lore@ki.se (K. Loré).

https://doi.org/10.1016/j.jim.2019.06.010
Received 27 February 2019; Received in revised form 19 May 2019; Accepted 5 June 2019
Available online 10 June 2019
0022-1759/

immunohistology and flow cytometry. Flow cytometry requires tissues to be processed into suspensions, which enables each cell to be analysed separately at the expense of spatial information and tissue architecture. In contrast, immunohistological analysis allows for the evaluation of intact tissue structures but the method can be more subjective and only one section of the tissue is analysed. There are also substantial differences in how GC data acquired by immunohistology are quantitatively analysed and presented in different studies, which makes comparing results difficult (Mastelic Gavillet et al., 2015; Vargas-Inchaustegui et al., 2016; Wray-Dutra et al., 2018; Gibson-Corley et al., 2012).

There is limited knowledge on how data compare between immunohistology and flow cytometry for GC analysis. Information about this is therefore warranted to facilitate the interpretation of data between studies and data presentation in future studies. The aim of this study was to directly compare GC data generated by flow cytometry and immunohistology using the same LN samples in order to evaluate previously reported methods for data analysis and to establish a strategy that would allow for direct comparison between the methods and thereby different studies and laboratories. In addition, since flow cytometry is generally regarded as a reproducible detection method, correlations between analysis methods by immunohistology and flow cytometry would indicate robustness in the analysis method by immunohistology. Of note, we intentionally used simple protocols of either method and applied available free software for image analysis so that the methods would be feasible for the majority of laboratories.

2. Materials and methods

2.1. Sample collection

This study was approved by the Local Ethical Committee on Animal Experiments. Indian rhesus macaques were housed at the Astrid Fagraeus laboratory at Karolinska Institutet in accordance with guidelines of the Association of Assessment and Accreditation of Laboratory Animal Care. Procedures were performed abiding to the provisions and general guidelines of the Swedish Animal Welfare Agency. Animals were anaesthetized with ketamine 10–15 mg/kg and medetomidine 0.05 mg/kg administered intramuscularly. Mesenteric LNs were collected at euthanasia and were immediately placed in RPMI (Gibco, Stockholm, Sweden), to be processed within 3 h.

2.2. LN processing

LNs were cleaned from fat and cut in half. One half was submerged in optimal cutting temperature (OCT) media compound (Tissue-Tek) on a plastic mould and placed on dry ice, before being brought to −80 °C for storage 2 h later. The other half was minced using surgical scissors and then filtered through 70 μm cell strainers as previously described (Frank Liang et al., 2017). Cells were then transferred into cryovials at a maximum of 25 million cells per ml of freezing media (10% DMSO diluted in fetal calf serum), cryovials were transferred into Mr. Frosty™ containers (Thermo Scientific™), which were stored in a −80 °C freezer.

2.3. Analysis of GCs by immunohistology

LNs embedded in OCT blocks were brought from −80 °C to −20 °C for 30 min to thaw. Seven μm sections were obtained using a CryoStar™ NX70 Cryostat. Tissues were allowed to adhere to Superfrost Plus™ slides (ThermoFisher) for 15 min before being fixed for 15 min in 2% formaldehyde solution, diluted in phosphate buffer saline (PBS). Tissues were washed in PBS and then permeabilized in tris-buffered saline with 0.1% saponin and 1% HEPES buffer (permwash with pH 7.4), with 1% fetal calf serum for blocking. After 30 min of blocking, tissues were incubated with primary antibodies overnight in 4 °C. For each LN, the first section was stained with CD3 (DAKO), anti-Ki67 (BD) and anti-PD1 (R&D systems) for the detection of GCs and a consecutive section was stained for anti-CD3 and anti-CD20 (BD) to quantify B cells (Supplementary Table I). Anti CD35 (BD), IgD (Southern Biotech) and BCL6 (BD) were used on separate sections to validate the staining strategy (Supplementary Table I). This was followed by blocking for 30 min with 1% donkey serum diluted in permwash. Endogenous biotin was blocked with avidin/biotin block (Vector Labs) according to manufacturer's instructions before the addition of each biotinylated secondary antibody (biotinylated donkey anti- rabbit, goat or mouse, Jackson Immuno Research). Antibodies were fluorescently labelled by a 30-minute incubation with streptavidin-conjugated Alexa Fluor 405/488/555/647 (Invitrogen). Coverslips were mounted using ProLong™ Diamond antifade mountant (Invitrogen™) according to manufacturer's instructions. Images were acquired using a Nikon Eclipse Ti-E confocal microscope. Tiled images (RGB TIFF files with CD3 in blue, PD1 in green and Ki67 in red), of LNs were analysed using CellProfiler™ v2.2.0, a Broad Institute product, on a Macbook Pro, macOS Sierra version 10.12.3. GCs were defined as clusters of $CD3^+PD1^+$ cells and $CD3^-Ki67^+$ cells similar to previous studies of other groups (Vargas-Inchaustegui et al., 2016; Hong et al., 2014; Kim et al., 2014; Petrovas et al., 2012). We did not use a nuclear stain such as DAPI in order to maintain a three-colour panel for simplicity and to enable all channels to fit within the RGB TIFF files used by CellProfiler™. A quadruple staining was performed to verify that $CD3^-Ki67^+$ cells were $CD20^+$ (B cells), for this a biotinylated anti-CD20 antibody (Abcam) was used in combination with CD3, PD1 and Ki67 (Supplementary Table I). Before analysis, accuracy of cell detection by the program was evaluated by ocular inspection of the original image compared to an image with the counted cells in several LN samples. The same GC analysis pipeline was used for all the data to enable an accurate comparison between the methods in the study. However, as the intensity of stainings vary between laboratories, the pipeline may need to be adjusted accordingly. For instance, the threshold levels for detection in modules 36–41 (IdentifyPrimaryObjects) may need to be increased or decreased.

Since it takes considerable time to manually merge all the data from the excel spreadsheets generated by CellProfiler and make the appropriate normalizations (e.g. divide total GC area by lymph node area), we developed a JAVA-based software named Lymf.jar that merges all the files. The CellProfiler™ pipeline and JAVA software Lymf.jar are available with detailed instructions at: https://github.com/Gustafhanslindgren/Comparative-analysis-of-the-germinal-center-response-by-flow-cytometry-and-immunohistology. Two videos of GC Z stacks are also provided in the link to show the absence of cell overlap. Also, an instruction video is available at: https://ki.box.com/s/yacofg7i4rukc9upn4ka5tps40hiccj6.

2.4. Analysis by flow cytometry

Cryovials were thawed in a 37 °C water bath and cells were immediately transferred to 10 ml complete media (10% FCS and 1% penicillin/streptomycin/glutamine diluted in RPMI, Gibco, Stockholm, Sweden). After washing twice, cells were counted and 2.5 million cells were transferred to separate tubes for staining. Cells were stained with LIVE/DEAD fixable blue (Invitrogen) according to manufacturer's instructions. The viability of the cells was 70–90%. This was followed by surface staining for 20 min with a panel of antibodies (Supplementary Table I). After washing, cells were permeabilized using a transcription factor buffer set (BD) according to manufacturer's instructions. Cells were subsequently stained for 20 min with intracellular markers (Supplementary Table I). After washing, cells were resuspended in 1% paraformaldehyde and approximately 1 million events were acquired using a LSRFortessa™ (BD). Data files were analysed using FlowJo software version 9.7.6.

2.5. Statistical analysis

Statistical analysis was performed using Prism Version 6.0

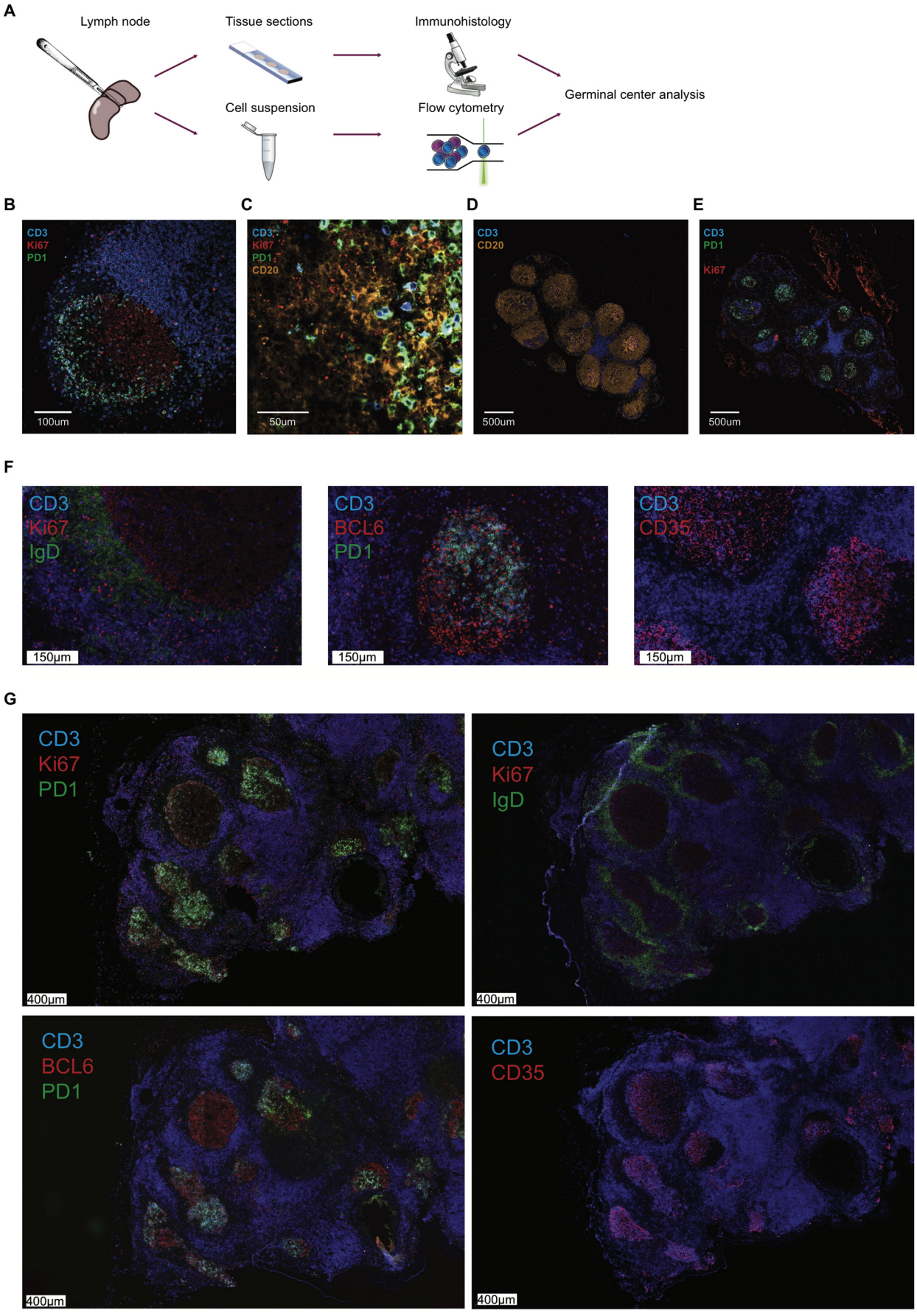

(caption on next page)

Fig. 1. Detection of germinal centers by immunohistology.
A) Study outline showing LN divided in two, each half was randomly assigned to either flow cytometry or immunohistology. B) GC staining using anti-CD3 (blue), anti-PD-1 (green), anti-Ki67 (red). C) GC staining with the addition of anti-CD20 (orange). D) Tiled image of LN stained for CD3 (blue) and CD20 (orange). E) Tiled image of LN stained for GCs using CD3 (blue), PD-1 (green) and Ki67 (red). F) High magnification images showing staining quality for IgD, BCL6 and CD35 respectively. G) Side by side comparisons using different combinations of CD3, PD1, Ki67, BCL6, IgD and CD35 for the detection of GCs. (For interpretation of the references to color in this figure legend, the reader is referred to the web version of this article.)

(GraphPad). All statistics were performed using Spearman's rank correlation.

3. Results

3.1. Immunohistology for CD3, PD1 and Ki67 enables simple detection of GCs

As mentioned above, while GCs are frequently analysed by either flow cytometry or immunohistology, data directly comparing the two methods is largely lacking. To bridge this knowledge gap, we performed a comparison of the two methods using LNs collected from rhesus macaques, since their immune cells and tissue architecture highly resemble that of humans and the same markers can thus be used for identification of GCs. Eighteen mesenteric LNs from seven rhesus macaques were divided into two pieces. Mesenteric LNs were chosen since they often contain GCs at steady state. One piece was processed for flow cytometry and the other for immunohistology (Fig. 1A). The LN pieces to be analysed by immunohistology were snapfrozen in OCT media and sections of the OCT blocks were stained and imaged. The donor-matched LN pieces were processed into cell suspension, frozen and later stained and analysed by flow cytometry.

For the cryosections, we used a combination of anti-CD3, anti-PD-1 and anti-Ki67 antibodies for identification of GCs (Fig. 1B) similar to what we have reported earlier (Frank Liang et al., 2017; Martinez-Murillo et al., 2017; Lindgren et al., 2017). We identified T_{FH} cells by CD3 and PD-1 expression and GC B cells by Ki-67 expression and lack of CD3, allowing for a simple approach using a limited but specific set of markers for detection of GCs. We confirmed that $CD3^-Ki67^+$ cells represented GC B cells by their expression of CD20 (Fig. 1C). Tiled images of entire LN sections stained for CD3 and CD20 (Fig. 1D) or CD3, PD-1 and Ki67 (Fig. 1E) were acquired with a motorized confocal microscope for subsequent computer analysis. We validated our staining strategy by testing additional markers that define GCs and their borders. IgD was used to specifically identify the mantel zone and the border of the GC, as previously described (Amodio et al., 2018) (Fig. 1F). BCL6 was used to detect T cells and B cells with a GC phenotype (Fig. 1F). CD35 mainly stains follicular dendritic cells in follicles and GCs (Fig. 1F). Although IgD, BCL6 and CD35 were useful markers for the detection of GCs and their orientation in the tissue, the area of the GCs could be defined in a similar fashion with CD3, PD1 and Ki67 together (Fig. 1G). One advantage with the combination of CD3, Ki67 and PD1 is also that these markers allow for enumeration of T_{FH} cells and GC B cells, which facilitates comparison to flow cytometry data.

Images were analysed with CellProfiler™ software using a customized set of algorithms operating within the program. In CellProfiler™, GCs were encircled manually and the $CD3^-Ki67^+$ cells (GC B cells) and $CD3^+PD\text{-}1^+$ (T_{FH} cells), respectively, were counted by the software (Fig. 2A). Total $CD3^+$ and $CD20^+$ cells were also counted by the software. Image analysis was performed after confirming by ocular inspection in a few control LNs that the software accurately identified the cell types. CellProfiler™ provides data on several parameters including the total number of each cell type counted in each analysed section and the number of these cells within each individual GC. To streamline the analysis, we developed a Java software to merge and organize all excel spreadsheets produced by CellProfiler™ (Fig. 2B).

We hypothesized that if GCs were correctly encircled, the area of the GC should correlate with the contents of the GC, i.e. GC B and T_{FH} cells. In line with this, there was a strong correlation between the GC area and the number of T_{FH} cells within each GC ($p < .0001$ $r = 0.9163$) as well as the GC area and the number of GC B cells ($p < .0001$ $r = 0.8933$) (Fig. 2C-D). There was also a significant albeit less strong correlation between the number of GC B cells and T_{FH} cells within individual GCs ($p < .0001$ $r = 0.7197$) (Fig. 2E). This could be due to the random orientation of the GCs between sections, resulting in various degrees of assessed dark versus light zones. The dark zone contains more $Ki67^+$ GC B cells and the light zone more T_{FH} cells, which would affect the correlations between GC B or T_{FH} cells with the GC area. However, this could be adjusted by instead combining the number of T_{FH} cells and GC B cells within a GC for the comparison with the GC area, which resulted in a strong correlation ($p < .0001$ $r = 0.9758$) (Fig. 2F). The total number of GC B cells and T_{FH} cells within each section also correlated well ($p < .0001$ $r = 0.8968$) (Fig. 2G). From this exercise, we concluded that the strategy for identification of GCs in the tissue sections was accurately performed.

3.2. Specific detection of T_{FH} cells and GC B cells by flow cytometry using a limited number of markers

For flow cytometry, we employed a staining protocol and gating strategy using nine antibodies for simultaneous identification of GC B cells and T_{FH} cells (Fig. 2H) (Supplementary Table I). From live singlet cells, $CD3^+CD20^-$ T cells and $CD3^-CD20^+$ B cells were separated. GC B cells were identified from the B cell population by Ki67 and BCL6 expression. T_{FH} cells were identified in the $CD4^+$ T cell populations by expression of PD1 and CXCR5 according to earlier work (Frank Liang et al., 2017; Lindgren et al., 2017; Havenar-Daughton et al., 2016b). We have earlier reported that T_{FH} cells identified with this gating strategy are exclusively found within the central memory compartment (Liang et al., 2017). Since GC B cells and T_{FH} cells are abundant in LNs but rare in the circulation, we validated the gating strategy by performing the same staining in peripheral blood mononuclear cells (PBMCs) for comparison (Fig. 2H). To further confirm that T_{FH} cells in LNs were correctly identified, their expression of ICOS was compared to that of non-T_{FH} T cells (Fig. 2I). The frequency of T_{FH} and GC B cells detected by flow cytometry correlated strongly, ($p < .0001$ $r = 0.9076$) (Fig. 2J) in line with earlier reports (Havenar-Daughton et al., 2016b).

3.3. Correlation of GC cell numbers by immunohistology and flow cytometry

With both methods established, we evaluated multiple ways to analyse GCs to determine analysis strategies where flow cytometry and immunohistology can generate comparable data. In immunohistology it is common to report GC activity as the number of GCs per LN, however the presence of small unspecific GCs can easily skew the data (Mastelic Gavillet et al., 2015; Gibson-Corley et al., 2012; Lofano et al., 2015). It can be hard to determine the number of GCs in an exact way, since GCs in close proximity to each other may be hard to discriminate (Fig. 3A). Also, the minimal number of T_{FH} cells and GC B cells that qualify as a GC is subjective (Fig. 3A). Consequently, if only the total number of GCs are used as a read-out, a LN with for example four large GCs will score lower than a LN with six small GCs. In addition, if the average GC size is used as a measurement, a LN with five large and ten small GCs might score lower than a LN with four medium-sized GCs. Hence, although the number of GCs can be of value in some studies, other ways of GC

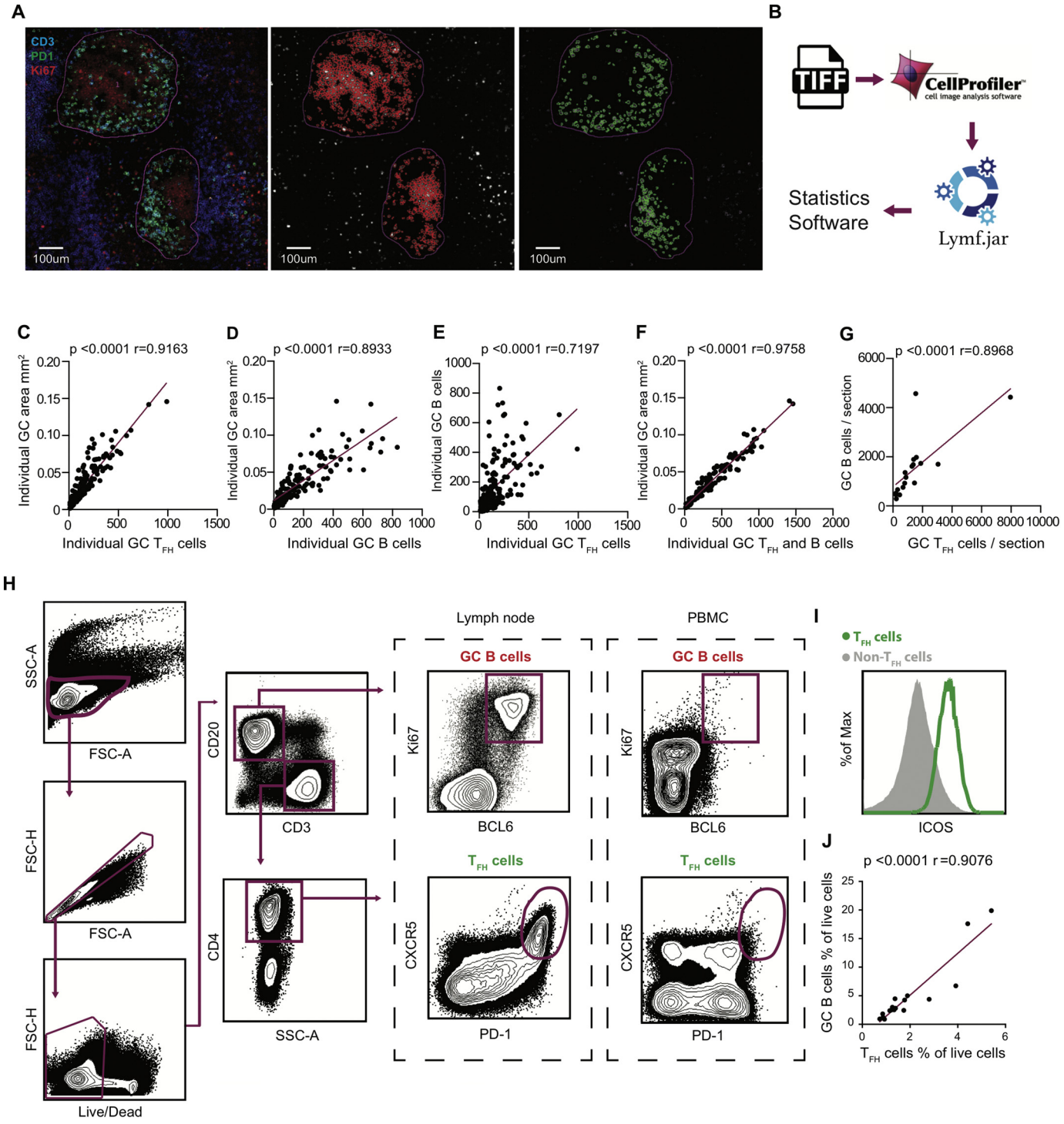

Fig. 2. Quantitative analysis of germinal centers by immunohistology and flow cytometry.
A) Example of GCs being manually encircled in CellProfiler™ and subsequent cell counting of $CD3^{-}Ki67^{+}$ (GC B) cells (red) and $PD1^{+}$ T cells (green) by the program. B) Illustration of data processing workflow C) Correlation between GC area and T_{FH} cells within individual GCs D) Correlation between GC area and GC B cells within individual GCs. E) Correlation of GC B cells and T_{FH} cells within individual GCs. F) Correlation between GC area and the combined number of GC B and T_{FH} cells within individual GCs. G) Correlation between total GC B cells and total T_{FH} cells per section. GC analysis performed on LN cells in suspension by flow cytometry using extracellular and intracellular staining. H) Gating strategy for the detection of GC B cells ($Ki67^{+}BCL6^{+}$) and T_{FH} cells ($CXCR5^{+}PD\text{-}1^{+}$). I) Expression of ICOS in T_{FH} cells and non-T_{FH} T cells. J) Correlation between GC B cells and T_{FH} cells measured by flow cytometry. (For interpretation of the references to color in this figure legend, the reader is referred to the web version of this article.)

analysis are often preferable. Regardless, the number of GCs cannot be determined by flow cytometry since GC B cells and T_{FH} cells are mixed in cell suspensions for this analysis. Instead, % GC area of section area or the frequency of GC cells in relation to other cells of all the GCs combined by immunohistology can be compared with data produced by flow cytometry. We therefore tested different data analysis techniques to try to determine ways to draw comparable conclusions between the two detection methods.

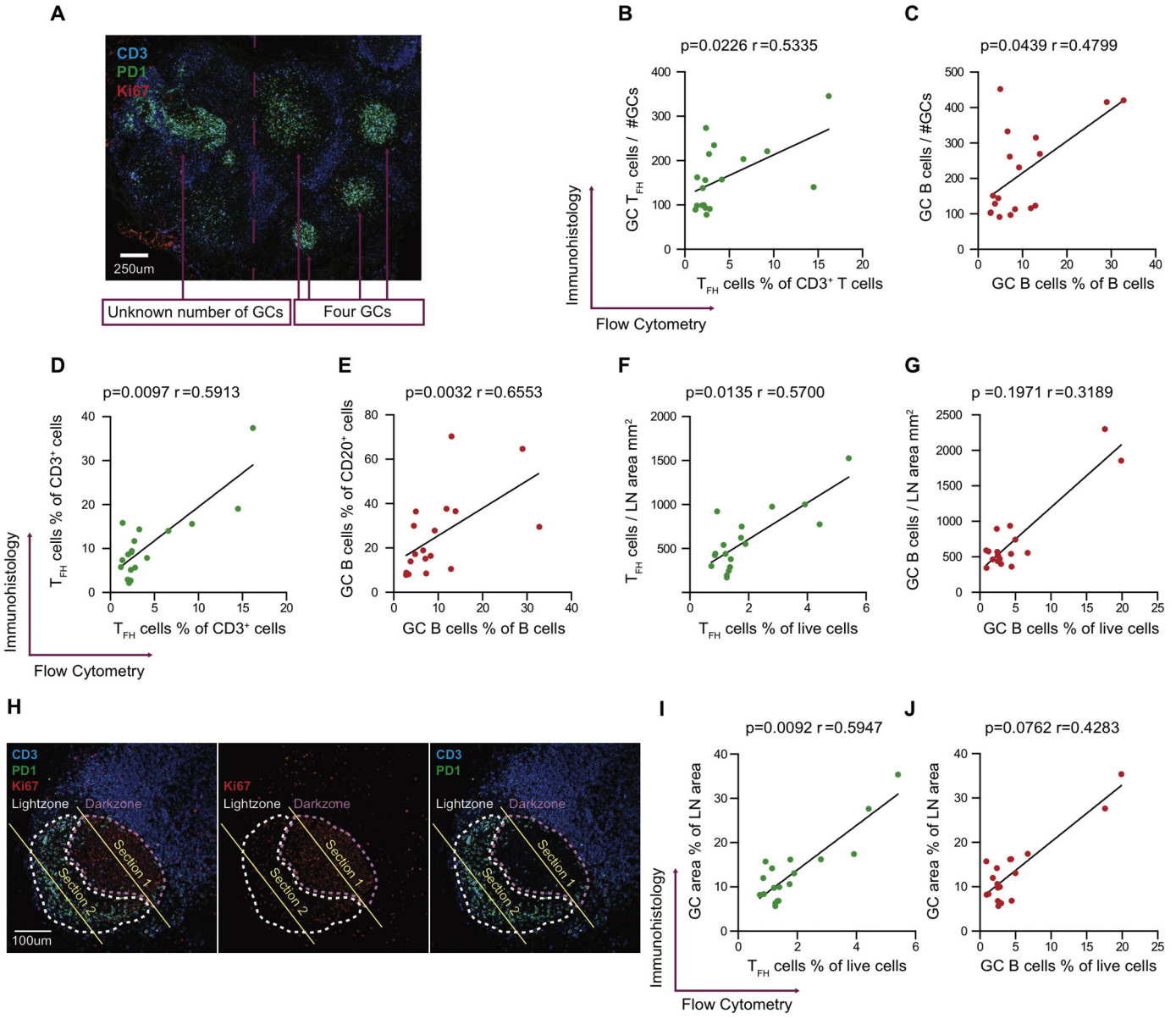

Fig. 3. Comparison of germinal center cell numbers or area by immunohistology and flow cytometry.
Correlations between immunohistology and flow cytometry within matched LNs, where each data point represents one LN. A) LN section stained for GCs illustrating the difficulty in defining the precise number of GCs B) Correlation between T_{FH} cells per GC and T_{FH} cells % of CD3 T cells by flow cytometry. C) Correlation between GC B cells per GC and GC B cells % of B cells by flow cytometry. D) Correlation between the number of T_{FH} cells % of CD3$^+$ T cells by immunohistology and T_{FH} cells % of CD3 T cells by flow cytometry. E) Correlation between the number of Ki67$^+$ GC cells % of CD20$^+$ B cells by immunohistology and GC B cells % of B cells by flow cytometry. F) Correlation between the number of T_{FH} cells per LN mm^2 and T_{FH} cells % of live cells by flow cytometry. G) Correlation between the number of Ki67$^+$ GC cells per LN mm^2 and GC B cells % of live cells by flow cytometry. H) LN section stained for GCs with marked dark and light zone followed by the same image with either CD3 and PD1 channels or Ki67 channel removed, to display cell density within compartment of the GC. I) Correlation between the % of GC area in LN sections and T_{FH} cells % of live cells by flow cytometry. J) Correlation between the % of GC area in LN sections and GC B cells % of live cells by flow cytometry.

We first compared the most commonly used read-outs for immunohistology and flow cytometry, respectively. Data generated by flow cytometry is typically presented as % of live cells or % of the parent population. We therefore first compared these values to several different normalization methods for immunohistology data. We normalized the number of T_{FH} cells or GC B cells in immunohistology by either the number of GCs in the section, the parent cells (CD3$^+$ or CD20$^+$) or the total LN area and compared the data to matching data from the other half of the LN obtained by flow cytometry (Fig. 3B-G). T_{FH} cells normalized by the number of GCs as detected by immunohistology were found to correlate moderately with T_{FH} cells (% out of total CD3$^+$ T cells) detected by flow cytometry ($p = .0226$ $r = 0.5335$) (Fig. 3B). Similar results were found for GC B cells normalized by the number of GCs by immunohistology when correlated to GC B cells (% out of total CD20$^+$ B cells) by flow cytometry ($p = .0439$ $r = 0.4799$) (Fig. 3C). Stronger correlations were found when instead using % T_{FH} cells or GC B cells out of parent population as means of normalizing immunohistology data. T_{FH} cells (% out of CD3$^+$ T cells) in tissue sections correlated well with T_{FH} cells (% out of CD3$^+$ T cells) obtained by flow cytometry ($p = .0097$ $r = 0.5913$) (Fig. 3D). GC B cells (% out of CD20$^+$ B cells) by immunohistology also correlated better with GC B cells (% out of CD20$^+$ B cells) by flow cytometry ($p = .0032$ $r = 0.6553$) (Fig. 3E).

We then tested whether the LN area measured by immunohistology resembled the total number of live cells measured by flow cytometry and would therefore be a good parameter for normalization. T_{FH} cells

normalized by the LN area by immunohistology showed a good correlation with T_{FH} cells (% out of live cells) by flow cytometry ($p < .0135$ $r = 0.5700$) (Fig. 3F). The total number of GC B cells normalized by LN area compared with GC B cells (% out of live) by flow cytometry had two outliers in our data set and did not correlate, however both outliers had high values for both immunohistology and flow cytometry ($p < .1971$ $r = 0.3189$) (Fig. 3G).

Another common method in immunohistology is to present the data as the combined area of all GCs (Martinez-Murillo et al., 2017; Wang et al., 2014; Ma and Ross, 2009). However, as mentioned above, for this analysis it is most rational to normalize the combined GC area by the total LN area being analysed. The structure of a GC is not uniform and a section of a LN may cut through the dark zone, light zone or both. Sections that mainly go through the dark zones of GCs will give a lower number of T_{FH} cells than a section of mainly light zones from the same LN (Fig. 3H). This phenomenon would influence data on the specific cell numbers measured but not the GC area, which is a potential advantage of this type of analysis. However, since the number of GC B cells and T_{FH} cells in each section correlated well (Fig. 2G) random section orientation of dark zone/light zone is unlikely to substantially influence the data. Still, we hypothesized that the size of the GC might reliably depict how many T_{FH} or GC B cells each GC contains and thus correlate with flow cytometric data. We found that the GC area normalized by total LN area correlated well with T_{FH} cells (% out of live) measured by flow cytometry ($p < .0092$ $r = 0.5947$) (Fig. 3I). However, the GC area normalized by LN area did not correlate with GC B cells (% out of live) measured by flow cytometry ($p = .0762$ $r = 0.4283$) (Fig. 3J).

To verify that our immunohistology results were reproducible, we analysed two additional sections for six of the LNs. These sections were 100 µm and 200 µm deeper into the LN (Supplementary Fig. 1A-C). Additionally, an entire tonsil was sectioned and analysed for GC areas to asses GC variability throughout the tissue (Supplementary Fig. 1D-E). There were variations in the total GC area between sections but this could be corrected by normalizing GC area by the total section area, which showed that the result of one section was often representative.

In conclusion, our findings suggest that data obtained by immunohistology and flow cytometry are best compared when data are presented as % GC B cells out of total $CD20^+$ B cells or % T_{FH} cells out of total $CD3^+$ T cells. The area of all GCs normalized by section area in immunohistology can also be suitable to use for comparisons to data on T_{FH} cells % of live cells from flow cytometry. Noteworthy is that although the measurement of GC area may be more subjective than measuring specific cells, it does not require automatic counting of cells and is less sensitive to errors by the software and to fluctuations in the staining intensity. Implementing one of these means of analysis would facilitate the comparison of data generated between the two methods.

3.4. Immunohistology and flow cytometry are comparable methods for GC analysis with separate advantages

To provide a visual representation of data from the two methods, examples of flow cytometry graphs and their respective LN image tiles are shown in Fig. 4. Two large and two small LNs with either low or high degree of GC activation are shown. Cell numbers shown in the graphs are % of parent cells. The T_{FH} and GC B cell populations are encircled in green and red respectively. The matched LN sections are presented below at the same magnification (Fig. 4). Regardless of the size of the LN section, the proportion of GCs as seen by immunohistology is comparable to the GC cell numbers (% of parent) measured by flow cytometry, especially T_{FH} cell numbers.

An aspect of this study was not only to define an analysis method that could be used to compare findings across studies, but also to reflect on relative advantages with each method. We have noted some advantages and disadvantages of each method in Table 1. In terms of time spent, data collection by flow cytometry usually takes one day, while collecting the same data by immunohistology is often more time-consuming. Since LNs are processed into suspension for flow cytometry, a representative value for the whole LN is obtained, unless fine needle aspiration sampling was performed which analyses a part. In contrast, data analysed by immunohistology can be more variable depending on the section that is stained. In this study, we have demonstrated that GC B cell or T_{FH} cell numbers normalized by total B cells or T cells, respectively, or total GC area normalized by section area, most closely resembles data from flow cytometry. As has been previously mentioned, immunohistology offers a clear advantage over flow cytometry in that it preserves spatial information and tissue architecture, which is essential for many studies. Tissues embedded in paraffin or cryo-media can be stored and reused multiple times, which offers further opportunities to address new questions. Although the modern staining procedures, reagents and equipment allow for multiple markers by immunohistology, the development of such panels can often be difficult and time consuming (Couillault et al., 2018). In flow cytometry, panels with many markers are routinely used in many laboratories and new cytometers such as the BD FACSymphony™ has the potential to analyse up to 50 parameters at a time, although such large panels will also require substantial optimization. Taken together, each method offers distinct advantages and the data presented here proposes ways to present GC data to make results generated by immunohistology and flow cytometry comparable.

4. Discussion

Direct comparison between flow cytometry and immunohistology, the two main methods of GC analysis, is lacking. Additionally, while the methods for quantitative analysis of GCs by flow cytometry are relatively established, there is little consensus between studies on how to quantify GC activity by immunohistology. This creates a problem when interpreting results between the two methods and between different methods of immunohistology analysis. Other methods for the analysis of GCs such as live imaging or histo-cytometry have recently emerged as useful tools for gaining detailed insight into the GC response, our paper however focuses on immunohistology and flow cytometry exclusively since these methods are most widely applied (Amodio et al., 2018; Gerner et al., 2012; Schwickert et al., 2011). Previous studies have compared flow cytometry to histo-cytometry, which applies algorithms on high resolution confocal images to acquire data-sets similar to those acquired by flow cytometry (Gerner et al., 2012). Using bone marrow chimeras and adoptive cell transfer in mice, dendritic cell densities in contralateral LNs have been compared between histo-cytometry and flow cytometry methods, demonstrating both similarities of some cell types and disparities among others (Gerner et al., 2012). Histo-cytometry has since been used in studies to investigate GC cell subsets after vaccination in tonsils (Amodio et al., 2018). Another study validated the use of fine needle aspirates by comparing it to whole LN biopsies assessed by flow cytometry (Havenar-Daughton et al., 2016b). In the current study, we applied a similar comparison between immunohistology and flow cytometry in matched LNs in order to establish methods for data analysis that can display comparable data. From our findings, we propose that evaluating GC B or T_{FH} cell numbers normalized to total B cells or T cells is a representative way to demonstrate GC activity in a way where data can be compared between the two platforms. The proportion of GC cells found by immunohistology was considerably higher than by flow cytometry. One possible explanation for this is that flow cytometry provides analysis on the entire LN including the outmost edges, which might not contain many GCs. Another explanation is that GC cells might be more prone to dying during the freeze-thawing procedure than general T cells and B cells, which would reduce their proportions in flow cytometry compared to immunohistology. However, since all LNs were harvested and frozen to cell suspension in the same way, any disproportional loss of GC cells would apply to all flow cytometric samples and would therefore not

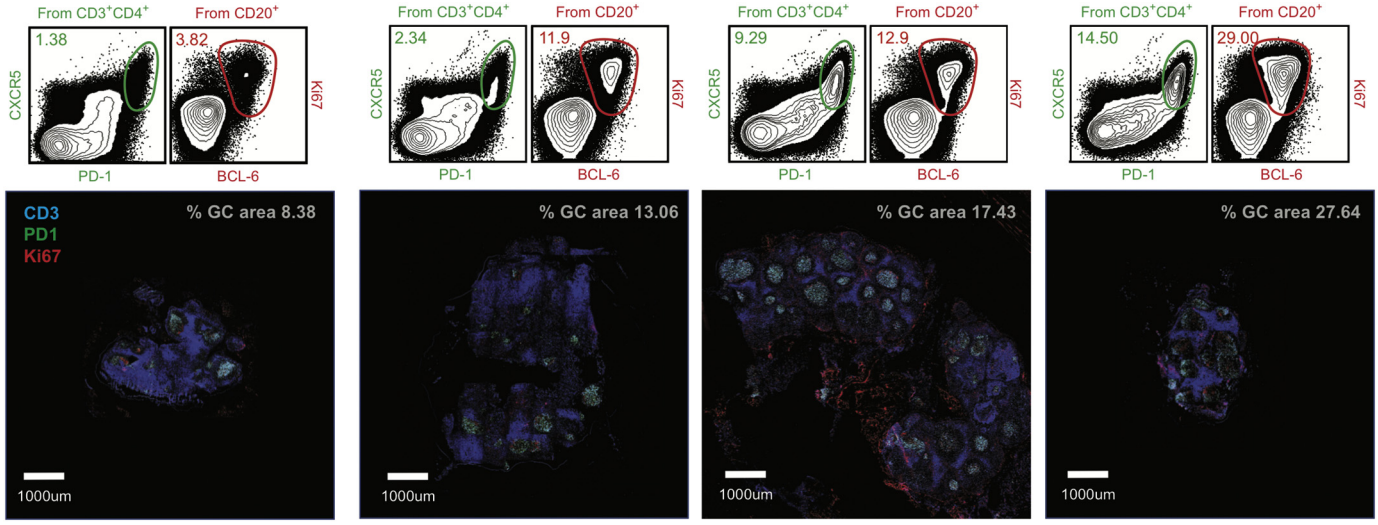

Fig. 4. A visual comparison of immunohistology and flow cytometry for the analysis of GCs.
Comparisons of flow cytometry graphs identifying GC B cells and T_{FH} cells and tissue sections from matched LNs stained for GCs. Two large and two small LNs with either high or low GC activity were picked to efficiently represent the data. Numbers show percent of parent.

Table 1
Relative advantages between immunohistology and flow cytometry for the analysis of GCs.

Aspect	Immunohistology	Flow cytometry
Time saving	No	Yes
Reproducible	Yes	Yes
Preserved tissue architecture	Yes	No
Sample reusability	Yes	No
Size of antibody panel	+	+ +

affect the correlations. GC area normalized by LN area also yields data comparable to flow cytometry, especially when compared to T_{FH} cells.

In vaccine studies, the induction of GC responses in otherwise nonreactive secondary lymphoid organs, such as vaccine-draining LNs, is a sign of robust vaccine responses (Havenar-Daughton et al., 2016b). However, in order to detect small differences between vaccine groups, the sensitivity and specificity of the method is highly important. Further, it is critical to be very selective when removing draining LNs for experimentation, due to LN scarcity and to avoid interfering with the ongoing immune response. The choice of analysis method is therefore crucial. The choice to use either immunohistology or flow cytometry to analyse GCs is often based on available equipment, expertise within the laboratory or desired data parameters such as tissue architecture (immunohistology) or multiple markers (flow cytometry). One concern when using immunohistology over flow cytometry is that enhanced GC responses can be missed due to difficulties in quantifying data, tissue heterogeneity and variations in the sectioning quality. In contrast, flow cytometry has several factors attributing to reproducible data, such as LNs being suspended into a homogenous solution, which ensures representative data, and well-established methods for quantifying the data, including gating strategies using FlowJo® software.

There are still distinct advantages to use immunohistochemistry. In the present study and previously, we have used CellProfiler™ to quantify the GC response in vaccine draining LNs (Frank Liang et al., 2017; Martinez-Murillo et al., 2017; Lindgren et al., 2017). This type of analysis enabled us to analyse each GC individually, which is not possible with flow cytometry, since all tissue architecture is lost. However, it has been shown that by using laser dissection on tissue sections, it is possible to analyse single GCs by flow cytometry, though this required genetically modified mice and may not be practical for extensive data collection (Jacobsen and Victora, 2017). Also, some cell types found within the GC such as follicular dendritic cells are hard to stain for by flow cytometry, whilst they are easily detectable by immunohistology (Heesters et al., 2017; Das et al., 2017). Extracellular molecules such as secreted cytokines are also hard to detect using flow cytometry and information on their proximity to specific cell types is lost, while this can be addressed by immunohistology. Additionally, while cells frozen for flow cytometry are single use only, tissues embedded in paraffin or cryo-media can be stored and reused multiple times, which offers further opportunities to address new research questions.

Given the distinct advantages and disadvantages of each method, the current study aimed to establish a method for drawing comparable conclusions between studies and selected methods. This would allow different laboratories to choose the method that best fit their needs, while still allowing for comparisons between studies. Since the number of GCs are considered in many studies, we used the number of GCs to normalize the total amount of GC B and T_{FH} cells and correlated to data acquired with flow cytometry and found weak correlations (Hong et al., 2014; Lofano et al., 2015; Wang et al., 2014). As described above, separating GCs that are in close proximity can be difficult, and defining the precise number of T_{FH} cells and GC B cells comprising a GC by immunohistology is often arbitrary. Future implementation of sophisticated algorithms or artificial intelligence could further enable for autonomous detection of GCs by the computer software, which would save time and increase reproducibility of results. Also, information on the number of GCs is not revealed by flow cytometry. We suggest that individual GC data either be considered a unique finding of immunohistology, that should not be directly compared to flow cytometry data, or that alternative ways of presenting immunohistology data are used as presented below.

Both T_{FH} cells normalized by $CD3^+$ cells and GC B cells normalized by $CD20^+$ cells correlated well with flow cytometry data. Additionally, GC area normalized by section area correlated well with data from flow cytometry, especially T_{FH} cells. Ultimately, based on our findings, either method is appropriate to measure the GC response and the choice should be based on the specific research questions and available expertise, but implementing the proposed means of analysis would facilitate the comparison of data between the two methods.

Supplementary data to this article can be found online at https://doi.org/10.1016/j.jim.2019.06.010.

Acknowledgements

The authors wish to thank Drs. Mats Spångberg and Bengt Eriksson and their staff at the Astrid Fagraeus laboratory for excellent animal care and expertise. We would also like to thank Joel Holmberg for technical assistance. The study was supported by a grant from Vetenskapsrådet to KL. GL, SO and EAT are recipients of PhD student salary faculty grant from Karolinska Institutet.

Declaration of Competing Interests

The authors have no conflicts of interest to disclose.

References

Amodio, D., Cotugno, N., Macchiarulo, G., Rocca, S., Dimopoulos, Y., Castrucci, M.R., De Vito, R., Tucci, F.M., McDermott, A.B., Narpala, S., Rossi, P., Koup, R.A., Palma, P., Petrovas, C., 2018. Quantitative multiplexed imaging analysis reveals a strong association between immunogen-specific B cell responses and tonsillar germinal center immune dynamics in children after influenza vaccination. J. Immunol. 200, 538–550.

Choi, Y.S., Kageyama, R., Eto, D., Escobar, T.C., Johnston, R.J., Monticelli, L., Lao, C., Crotty, S., 2011a. ICOS receptor instructs T follicular helper cell versus effector cell differentiation via induction of the transcriptional repressor Bcl6. Immunity 34, 932–946.

Choi, Y.S., Kageyama, R., Eto, D., Escobar, T.C., Johnston, R.J., Monticelli, L., Lao, C., Crotty, S., 2011b. Bcl6 dependent T follicular helper cell differentiation diverges from effector cell differentiation during priming and depends on the gene Icos. Immunity 34, 932–946.

Couillault, C., Germain, C., Dubois, B., Kaplon, H., 2018. Identification of tertiary lymphoid structure-associated follicular helper T cells in human tumors and tissues. In: Dieu-Nosjean, M.-C. (Ed.), Tertiary Lymphoid Structures: Methods and Protocols. Springer New York, New York, NY, pp. 205–222.

Das, A., Heesters, B.A., Bialas, A., O'Flynn, J., Rifkin, I.R., Ochando, J., Mittereder, N., Carlesso, G., Herbst, R., Carroll, M.C., 2017. Follicular dendritic cell activation by TLR ligands promotes autoreactive B cell responses. Immunity 46, 106–119.

Domeier, P.P., Schell, S.L., Rahman, Z.S., 2017. Spontaneous germinal centers and autoimmunity. Autoimmunity 50, 4–18.

Doria-Rose, N.A., Joyce, M.G., 2015. Strategies to guide the antibody affinity maturation process. Curr. Opin. Virol. 11, 137–147.

Frank Liang, G.L., Sandgren1, Kerrie J., Thompson, Elizabeth A., Francica, Joseph R., Seubert, Anja, De Gregorio, Ennio, Barnett, Susan, O'Hagan, Derek T., Sullivan, Nancy J., Koup, Richard A., Seder, Robert A., Loré, Karin, 2017. Vaccine priming is restricted to draining lymph nodes and controlled by adjuvant-mediated antigen uptake. Sci. Transl. Med. 9.

Gerner, M.Y., Kastenmuller, W., Ifrim, I., Kabat, J., Germain, R.N., 2012. Histo-cytometry: a method for highly multiplex quantitative tissue imaging analysis applied to dendritic cell subset microanatomy in lymph nodes. Immunity 37, 364–376.

Gibson-Corley, K.N., Boggiatto, P.M., Bockenstedt, M.M., Petersen, C.A., Waldschmidt, T.J., Jones, D.E., 2012. Promotion of a functional B cell germinal center response after Leishmania species co-infection is associated with lesion resolution. Am. J. Pathol. 180, 2009–2017.

Havenar-Daughton, C., Lindqvist, M., Heit, A., Wu, J.E., Reiss, S.M., Kendric, K., Belanger, S., Kasturi, S.P., Landais, E., Akondy, R.S., McGuire, H.M., Bothwell, M., Vagefi, P.A., Scully, E., Investigators, I.P.C.P., Tomaras, G.D., Davis, M.M., Poignard, P., Ahmed, R., Walker, B.D., Pulendran, B., McElrath, M.J., Kaufmann, D.E., Crotty, S., 2016a. CXCL13 is a plasma biomarker of germinal center activity. Proc. Natl. Acad. Sci. U. S. A. 113, 2702–2707.

Havenar-Daughton, C., Carnathan, D.G., Torrents de la Pena, A., Pauthner, M., Briney, B., Reiss, S.M., Wood, J.S., Kaushik, K., van Gils, M.J., Rosales, S.L., van der Woude, P., Locci, M., Le, K.M., de Taeye, S.W., Sok, D., Mohammed, A.U., Huang, J., Gumber, S., Garcia, A., Kasturi, S.P., Pulendran, B., Moore, J.P., Ahmed, R., Seumois, G., Burton, D.R., Sanders, R.W., Silvestri, G., Crotty, S., 2016b. Direct probing of germinal center responses reveals immunological features and bottlenecks for neutralizing antibody responses to HIV Env trimer. Cell Rep. 17, 2195–2209.

Heesters, B.A., Van der Poel, C.E., Carroll, M.C., 2017. Follicular dendritic cell isolation and loading of immune complexes. In: Calado, D.P. (Ed.), Germinal Centers: Methods and Protocols. Springer New York, New York, NY, pp. 105–112.

Hong, J.J., Amancha, P.K., Rogers, K.A., Courtney, C.L., Havenar-Daughton, C., Crotty, S., Ansari, A.A., Villinger, F., 2014. Early lymphoid responses and germinal center formation correlate with lower viral load set points and better prognosis of simian immunodeficiency virus infection. J. Immunol. 193, 797–806.

Jacobsen, J.T., Victora, G.D., 2017. Microanatomical labeling of germinal center structures for flow cytometry using Photoactivation. In: Calado, D.P. (Ed.), Germinal Centers: Methods and Protocols. Springer New York, New York, NY, pp. 51–58.

Kim, E.J., Kwun, J., Gibby, A.C., Hong, J.J., Farris, A.B., 3rd, N.N. Iwakoshi, Villinger, F., Kirk, A.D., Knechtle, S.J., 2014. Costimulation blockade alters germinal center responses and prevents antibody-mediated rejection. Am. J. Transplant. Off. J. Am. Soc. Transplant. Am. Soc. Transplant Surg. 14, 59–69.

Kuppers, R., 2005. Mechanisms of B-cell lymphoma pathogenesis. Nat. Rev. Cancer 5, 251–262.

Liang, F., Lindgren, G., Sandgren, K.J., Thompson, E.A., Francica, J.R., Seubert, A., De Gregorio, E., Barnett, S., O'Hagan, D.T., Sullivan, N.J., Koup, R.A., Seder, R.A., Loré, K., 2017. Vaccine priming is restricted to draining lymph nodes and controlled by adjuvant-mediated antigen uptake. Sci. Transl. Med. 9.

Lindgren, G., Ols, S., Liang, F., Thompson, E.A., Lin, A., Hellgren, F., Bahl, K., John, S., Yuzhakov, O., Hassett, K.J., Brito, L.A., Salter, H., Ciaramella, G., Lore, K., 2017. Induction of robust B cell responses after influenza mRNA vaccination is accompanied by circulating hemagglutinin-specific ICOS+ PD-1+ CXCR3+ T follicular helper cells. Front. Immunol. 8, 1539.

Lofano, G., Mancini, F., Salvatore, G., Cantisani, R., Monaci, E., Carrisi, C., Tavarini, S., Sammicheli, C., Rossi Paccani, S., Soldaini, E., Laera, D., Finco, O., Nuti, S., Rappuoli, R., De Gregorio, E., Bagnoli, F., Bertholet, S., 2015. Oil-in-water emulsion MF59 increases germinal center B cell differentiation and persistence in response to vaccination. J. Immunol. 195, 1617–1627.

Ma, Y., Ross, A.C., 2009. Toll-like receptor 3 ligand and retinoic acid enhance germinal center formation and increase the tetanus toxoid vaccine response. Clin. Vaccine Immunol. 16, 1476–1484.

Martinez-Murillo, P., Tran, K., Guenaga, J., Lindgren, G., Adori, M., Feng, Y., Phad, G.E., Vazquez Bernat, N., Bale, S., Ingale, J., Dubrovskaya, V., O'Dell, S., Pramanik, L., Spangberg, M., Corcoran, M., Lore, K., Mascola, J.R., Wyatt, R.T., Karlsson Hedestam, G.B., 2017. Particulate Array of well-ordered HIV clade C Env trimers elicits neutralizing antibodies that display a unique V2 cap approach. Immunity 46 (804–817), e807.

Mastelic Gavillet, B., Eberhardt, C.S., Auderset, F., Castellino, F., Seubert, A., Tregoning, J.S., Lambert, P.H., de Gregorio, E., Del Giudice, G., Siegrist, C.A., 2015. MF59 mediates its B cell Adjuvanticity by promoting T follicular helper cells and thus germinal center responses in adult and early life. J. Immunol. 194, 4836–4845.

Mesin, L., Ersching, J., Victora, G.D., 2016. Germinal center B cell dynamics. Immunity 45, 471–482.

Petrovas, C., Yamamoto, T., Gerner, M.Y., Boswell, K.L., Wloka, K., Smith, E.C., Ambrozak, D.R., Sandler, N.G., Timmer, K.J., Sun, X., Pan, L., Poholek, A., Rao, S.S., Brenchley, J.M., Alam, S.M., Tomaras, G.D., Roederer, M., Douek, D.C., Seder, R.A., Germain, R.N., Haddad, E.K., Koup, R.A., 2012. CD4 T follicular helper cell dynamics during SIV infection. J. Clin. Invest. 122, 3281–3294.

Patrick Schaerli, K. W., Alois B. Lang,‡ Martin Lipp,§ Pius Loetscher, and Bernhard Moser. 2000. CXC chemokine receptor 5 expression defines follicular homing T cells with B cell helper function. J. Exp. Med. 192: 1553–1562.

Schwickert, T.A., Victora, G.D., Fooksman, D.R., Kamphorst, A.O., Mugnier, M.R., Gitlin, A.D., Dustin, M.L., Nussenzweig, M.C., 2011. A dynamic T cell–limited checkpoint regulates affinity-dependent B cell entry into the germinal center. J. Exp. Med. 208, 1243–1252.

Shi, J., Hou, S., Fang, Q., Liu, X., Liu, X., Qi, H., 2018. PD-1 controls follicular T helper cell positioning and function. Immunity. 49, 264–274.

Sobecki, M., Mrouj, K., Camasses, A., Parisis, N., Nicolas, E., Lleres, D., Gerbe, F., Prieto, S., Krasinska, L., David, A., Eguren, M., Birling, M.C., Urbach, S., Hem, S., Dejardin, J., Malumbres, M., Jay, P., Dulic, V., Lafontaine, D., Feil, R., Fisher, D., 2016. The cell proliferation antigen Ki-67 organises heterochromatin. Elife 5, e13722.

Vargas-Inchaustegui, D.A., Demers, A., Shaw, J.M., Kang, G., Ball, D., Tuero, I., Musich, T., Mohanram, V., Demberg, T., Karpova, T.S., Li, Q., Robert-Guroff, M., 2016. Vaccine induction of lymph node-resident simian immunodeficiency virus Env-specific T follicular helper cells in rhesus macaques. J. Immunol. 196, 1700–1710.

Victora, G.D., Nussenzweig, M.C., 2012. Germinal centers. Annu. Rev. Immunol. 30, 429–457.

Wang, C., Liu, P., Zhuang, Y., Li, P., Jiang, B., Pan, H., Liu, L., Cai, L., Ma, Y., 2014. Lymphatic-targeted cationic liposomes: a robust vaccine adjuvant for promoting long-term immunological memory. Vaccine 32, 5475–5483.

Willard-Mack, C.L., 2006. Normal structure, function, and histology of lymph nodes. Toxicol. Pathol. 34, 409–424.

Wray-Dutra, M.N., Chawla, R., Thomas, K.R., Seymour, B.J., Arkatkar, T., Sommer, K.M., Khim, S., Trapnell, C., James, R.G., Rawlings, D.J., 2018. Activated CARD11 accelerates germinal center kinetics, promoting mTORC1 and terminal differentiation. J. Exp. Med. 215, 2445–2461.